J. Membrane Biol. 172, 215–223 (1999)

The Journal of
Membrane
Biology

Ion Permeation and Block of $P2X_2$ Purinoceptors: Single Channel Recordings

S. Ding[1], **F. Sachs**[2]

[1]Department of Chemical Engineering and [2]Physiology and Biophysics, State University of New York at Buffalo, Buffalo, NY 14214, USA

Received: 3 May 1999/Revised: 23 August 1999

Abstract. $P2X_2$ purinoceptors are cation-selective channels activated by ATP and its analogues. Using single channel measurements we studied the channel's selectivity for the alkali metal ions and organic monovalent cations $NMDG^+$, $Tris^+$, TMA^+, and TEA^+. The selectivity sequence for currents carried by alkali metal ions is: $K^+ > Rb^+ > Cs^+ > Na^+ > Li^+$, which is *Eisenman* sequence IV. This is different from the mobility sequence of the ions in free solution suggesting there is weak interaction between the ions and the channel interior. The relative conductance for alkali ions increases linearly in relation to the *Stokes* radius. The organic ions $NMDG^+$, $Tris^+$, TMA^+ and TEA^+ were virtually impermeant. The divalent ions (Mn^{2+}, Mg^{2+}, Ca^{2+} and Ba^{2+}) induced a fast block visible as a reduction in amplitude of the unitary currents. Using a single-site binding model, the divalent ions exhibited an equilibrium affinity sequence of $Mn^{2+} > Mg^{2+} > Ca^{2+} > Ba^{2+}$.

Key words: ATP — Cations — Patch-clamp — Single channel

Introduction

Receptors activated by extracellular ATP and its analogues are known as P2 purinoceptors (Fredholm et al., 1997). They are classified into two families, P2Y and P2X. P2Y purinoceptors are G protein coupled receptors, whereas members of P2X family form ligand-gated cation channels (Abbracchio et al., 1996). Seven members of the P2X family, designated $P2X_{1–7}$, have been cloned and are readily expressed in heterologous cells such as *Xenopus* oocytes and HEK 293 cells (North & Barnard, 1997). The electrophysiological and pharmacological properties of the cloned receptors are similar to those of the native receptors. The protein topology of P2X purinoceptors suggests a structure with two hydrophobic transmembrane domains (M1 and M2), and both the C- and N-termini are located on the intracellular side. This structure differs from other ligand-gated channels, such as nicotinic acetylcholine receptors (nAChR) and ionotropic glutamate receptors, thus defining a novel structural motif for ligand-gated ion channels (Brake, Wagenbach & Julius, 1994; Nicke et al., 1998). $P2X_1$ and $P2X_3$ receptors expressed in *Xenopus* oocytes appear to assemble as trimers (Nicke et al., 1998), consistent with our previous study (Ding & Sachs, 1999*a*).

Most studies of cloned P2X receptors have focused on the primary structure and channel pharmacology based on whole cell currents, while only a small amount of work has been devoted to single channel properties. Single channel currents of $P2X_2$ receptors expressed in HEK293 cells have a chord conductance of ~30 pA at −100 mV, with symmetrical 145 mM Na^+, and inwardly rectify even in the absence of divalent ions (Ding & Sachs, 1999). A large excess open channel noise (SD ~30% of its mean amplitude) is a characteristic feature (Ding & Sachs, 1999*a*). Single channel currents from $P2X_1$ receptors expressed in *Xenopus* oocytes were reported to have a mean amplitude of ~2 pA at −140 mV and a chord conductance of 19 pS between −140 and −80 mV (Valera et al., 1994). The conductance for $P2X_1$, $P2X_2$ and $P2X_4$ channels expressed in Chinese hamster ovary (CHO) cells were about 18, 21, and 9 pS, respectively, at −100 mV, with 150 mM extracellular NaCl, but the openings of $P2X_3$ were not resolved (Evans, 1996). Given the flickery, 'bursting' character of the open state, the meaning of 'open channel conductance' remains unclear.

Although P2X receptors are nonselective cation channels, their conductances vary with different cations. Whole cell recordings show that the replacement of extracellular Na^+ by K^+ does not significantly affect the reversal potential of $P2X_2$ receptors, suggesting that Na^+

Correspondence to: F. Sachs

and K^+ have a similar permeability near 0 mV (Brake et al., 1994). However, at negative potentials the currents carried by Na^+ were larger than the currents carried by K^+. Similar results were reported for PC12 cells (Nakazawa et al., 1990). Based on reversal potential measurements of whole cell currents, the organic ions such as N-methyl-D-Glucamine ($NMDG^+$), Tris(hydroxylmethyl) aminomethane ($Tris^+$), and tetraethylammonium (TEA^+) have a very low permeability compared with Na^+ (Evans et al., 1996). Cation selectivity based on whole cell current recording may not be consistent with single channel conductance since the gating kinetics may vary with different cations (Akk & Auerbach, 1996). Therefore, it is necessary to measure single channel conductances directly.

P2X receptors are permeable to monovalent cations as well as divalents. The permeation of Ca^{2+} is of particular interest because of its role as a second messenger (Benham, 1990, 1992). The Ca^{2+} permeability of ATP-gated channels has been measured utilizing reversal potentials of whole cell currents, single channel recordings, and analysis of the ATP-induced rise in intracellular Ca^{2+} (Benham, Bouvier & Evans, 1991; Rogers & Dani, 1995; Evans et al., 1996; Virginio et al., 1998). However, since intracellular Ca^{2+} can modify the gating of many other channels, whole cell reversal potential measurements of Ca^{2+} permeability may not be trustworthy.

Although Ca^{2+} is probably permeant, the primary effect of extracellular Ca^{2+} is to reduce the current carried by Na^+. This Ca^{2+}-sensitivity of P2X single channel currents is different in different cells. In sensory neurons the estimated EC_{50} for pore blockade of Na^+ currents through P2X channels is ~100 μM, ~6 mM in PC12 cells (Krishtal, Marchenko & Obukhov, 1988; Nakazawa & Hess, 1993), 89 mM for $P2X_3$ receptors and 15 mM for $P2X_{2/3}$ receptors (Virginio et al., 1998). Other divalent cations, such as Mn^{2+}, Mg^{2+}, and Ba^{2+}, have similar effects with an order of potency of $Cd^{2+} > Mn^{2+} > Mg^{2+} > \approx Ca^{2+} > Ba^{2+}$ in PC12 cells (Nakazawa & Hess, 1993). Extracellular Mg^{2+} greatly reduces the whole cell currents of cloned $P2X_7$ receptors expressed in HEK 293 cells (Surprenant et al., 1996). While $P2X_2$ receptors were cloned from PC12 cells, these cells probably contain a mixed population of P2X isoforms, and may have different cellular regulation pathways from the heterotypic expression systems used here.

Recently it has been reported that application of ATP for tens of seconds causes a dilation of the pores of $P2X_2$ receptors expressed in HEK 293 cells. In whole cell recordings this effect is seen as increases in conductance and relative permeability for large cations (Virginio et al., 1999; Khakh et al., 1999). The dilation, however, has never been observed in patch experiments including these. The origin of the disparity with recording conditions remains to be resolved.

Here we have studied at the single channel level the ionic current selectivity of heterotypically expressed $P2X_2$ channels. The permeation selectivity sequence for alkali metal ions is: $K^+ > Rb^+ > Cs^+ > Na^+ > Li^+$. All of the organic ions we tested ($NMDG^+$, $Tris^+$, TMA^+ and TEA^+) had very small currents. Divalent cations reduced the single channel current amplitude in the order: $Mn^{2+} > Mg^{2+} > Ca^{2+} > Ba^{2+}$.

Materials and Methods

Electrophysiological Recording

Recordings were performed on HEK 293 cells stably transfected with $P2X_2$ purinoceptors (kindly provided by Dr. Annmarie Surprenant, Geneva Biomedical Research Institute) at room temperature. For electrophysiology experiments, the HEK 293 cells were cultured at 37°C for 1–2 days after passage. The medium for HEK 293 cells contained: 90% DMEM/F12, 10% heat inactivated fetal calf serum, and 300 μg/ml Geneticin (G418). The media were adjusted to pH 7.35 with NaOH and sterilized by filtration.

Currents activated by ATP were measured with a AXOPATCH 200B amplifier in whole cell and outside-out configurations, using standard patch-clamp techniques (Hamill et al., 1981). Recording pipettes were pulled from borosilicate glass (World Precision Instruments, Sarasota, FL) and coated with Sylgard, and had resistances of 10 ~ 20 MΩ.

The composition of the pipette solution was (in mM): 145 NaF, 11 EGTA, and 10 HEPES, pH 7.4. The bath solution and control perfusion solutions were the same and contained (in mM): 145 NaCl, 2 KCl, 1 $MgCl_2$, 1 $CaCl_2$, 11 glucose, and 10 HEPES, pH 7.4. For recordings performed on oocytes, the same solutions were used as on HEK 293 cells except that Na^+ was reduced to 100 mM in the internal and external solutions. In the study on the effect of different cations on channel conductance, we replaced the extracellular Na^+ by the test ions K^+, Rb^+, Cs^+, Na^+, Li^+, N-methyl-D-Glucamine ($NMDG^+$), Tris(hydroxylmethyl) aminomethane hydrochloride ($Tris^+$), tetramethylammonium chloride (TMA^+), and tetraethylammonium chloride (TEA^+), and other components remained the same. ATP was applied to outside-out patches by an ALA BPS-4 perfusion system (ALA Scientific Instruments, Westbury, NY). The perfusion solution was the same as the bath solution but with the addition of ATP and various ions. All chemicals were purchased from Sigma Chemical (St. Louis, MO).

The data were stored on videotape using a VR-10A digital data recorder (Instrutech, Great Neck, NY). The patch currents were filtered at 5 kHz and digitized at 10 kHz and the whole cell currents were filtered at 1 kHz and digitized at 2 kHz using a Labview data acquisition system (National Instruments).

Analysis

Mean amplitude of single channel currents carried by alkali metal ions was determined by fitting the all-points amplitude histogram *Gaussian* distributions. Because of their small amplitudes, single channel currents carried by organic ions were estimated by the Hidden Markov program SKM (www.qub.buffalo.edu) assuming a two-state model.

To go from currents to an intrinsic channel property such as permeability or conductance requires a model. Since there is no accepted common model, we have used various approximations. Chord conductances G were calculated according to Eq. 1:

$$G = i/(V - V_r) \quad (1)$$

where i is the single channel amplitude, V is the membrane potential and V_r a reversal potential. Because the channels have nonlinear conductances (the permeability is voltage dependent), whole cell current reversal potentials for the alkali ions were similar, and our measurements were made quite negative to the reversal potentials, we have used 0 mV as the reversal potentials for the alkali metal ions. The reversal potentials for organic ions were taken from Evans et al. (1996). The excess open channel noise (σ_{ex}) was computed as the rms difference between the variances of the open channel current and the shut channel current (Sivilotti et al., 1997).

Although divalent cations are permeant, the fraction of current carried by Ca^{2+} relative to the alkali ions is small (Evans et al., 1996). Consequently, in analyzing the blocking effect of Ca^{2+} we simply used the *Woodhull* equation for reversible single site binding (Woodhull, 1973):

$$I_b = I(0)/(1 + [M^{2+}]/K_d) \quad (2)$$

where I_b is current after block, $I(0)$ is current without block, $[M^{2+}]$ is the concentration of divalent ions, and K_d is the apparent dissociation constant.

We used Origin 5 (Microcal Software, Northhampton, MA) and Scientist (MicroMath Scientific Software) software to simulate and fit the data.

Results

Typical Single Channel Current

Figure 1*A* shows a typical single channel current carried by extracellular K^+, activated by 1.5 μM ATP at a membrane potential of −120 mV from a stably transfected HEK 293 cell. Channel openings appeared as flickery bursts with ill-defined conductance levels. The open channel current fluctuations have a much larger standard deviation (SD) than the closed channel, although each could be fit well with a single *Gaussian.* In Fig. 1*B*, the mean open channel current is 6.2 pA, equivalent to a chord conductance of 52 pS. The 'true' single channel current is significantly larger than the mean, since the excess noise appears to be made up of unresolved gating transitions to lower current states (Ding & Sachs, 1999). The standard deviations of the open and closed histograms are 1.65 and 0.24 pA, respectively, so that the excess open channel noise σ_{ex} is 1.63 pA, i.e., 26% of the mean current amplitude, similar to the values previously reported for sodium currents (Ding & Sachs, 1999). For the sake of simplicity, we will refer to the open channel current by its mean value, even though this is well below the peak.

Figure 2*A* shows single channel currents activated by 2 μM ATP at different holding potentials, using outside-out patches with symmetrical Na^+. At positive holding potentials, the currents became small and noisy, so that the unitary currents were not discernible. Occasionally we saw the overlapping of single channel currents due to the presence of multiple channels. The single channel *I–V* curve (Fig. 2*B*) between −120 to −50 mV exhibited inward rectification and the rapid fluctuations of current in the 'open' state were maintained at all potentials.

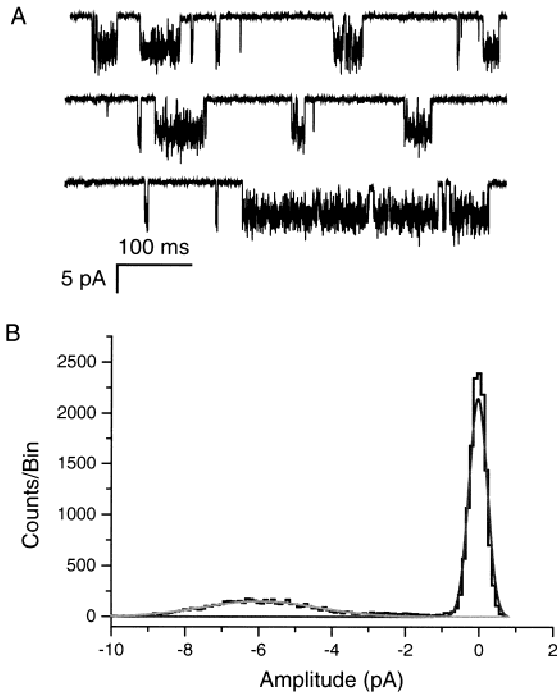

Fig. 1. Typical single channel currents from an outside-out patch of an HEK 293 cell. (*A*) The current was activated by 1.5 μM ATP at −120 mV with 140 mM extracellular K^+ in the presence of 1 mM extracellular Mg^{2+} and Ca^{2+} (inward current downward). The data were low-pass filtered at 5 kHz and digitized at 10 kHz. Note the large fluctuations in open channel current. (*B*) The all-points amplitude histogram of single channel currents from A (0.2 pA/bin). The distribution was fit by a sum of two *Gaussians* (solid line), with means of 0 and 6.2 pA. The standard deviation of the open state peak (SD = 1.65 pA) is much larger than that of the closed state (SD = 0.23 pA).

Channel Conductance Selectivity Based on Single Channel Recording

$P2X_2$ receptor ion channels are nonselective cation channels, but the conductance varies with the cation. To obtain information on ion selectivity, and to estimate the physical size of the $P2X_2$ channel pore, we measured single channel currents in HEK 293 cells using outside-out patches with NaF as the intracellular solution and K^+, Rb^+, Cs^+, Na^+, Li^+, $NMDG^+$, $Tris^+$, TMA^+ or TEA^+ as extracellular ions. Figure 3 shows the single channel currents activated by 2 μM ATP at −120 mV with different ions. The mean open channel currents are different with different alkali metal ions, but the flickering behavior is similar, suggesting that it does not arise from

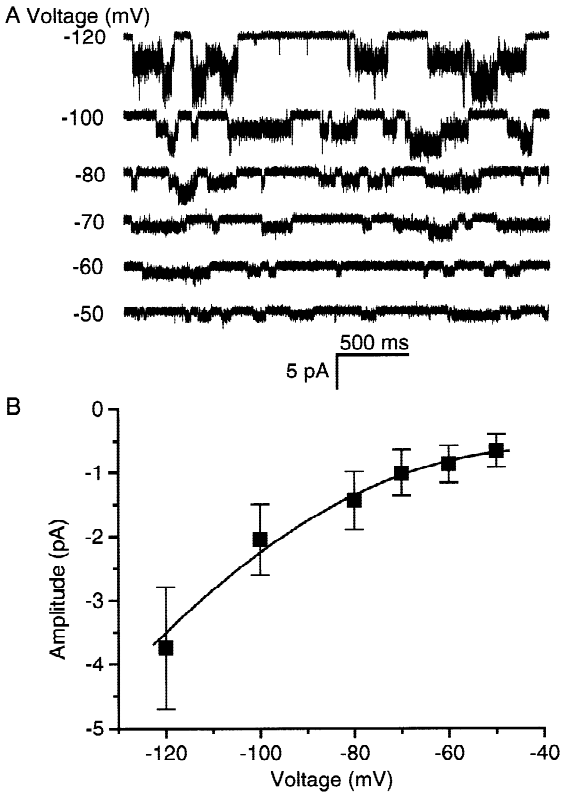

Fig. 2. The current-voltage (*I–V*) relationship of single channel currents. (*A*) Single channel currents of an outside-out patch from HEK 293 cells activated by 2 μM ATP at different membrane potentials in the presence of 1 mM extracellular Mg^{2+} and Ca^{2+} with symmetrical Na^+ solutions containing 145 mM extracellular NaCl/145 mM intracellular NaF. The data were filtered at 5 kHz and digitized at 10 kHz. All current traces in this figure are from the same patch. Note the overlap due to the opening of multiple channels. (*B*) Mean *I–V* relationship for single channel currents. The error bars indicate the excess open channel noise of the single channel currents from the all-points histograms. The single channel *I–V* relationship exhibits inward rectification despite exposure to identical Na^+ solutions across the patch. The solid line is simply a spline fit to the single channel amplitudes.

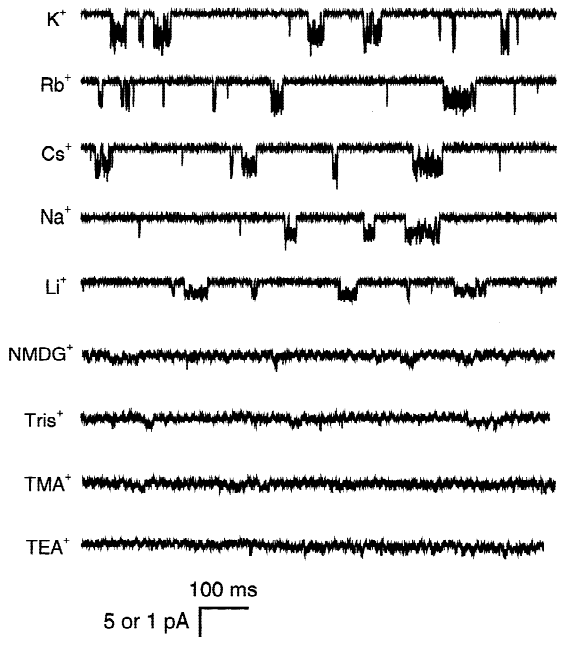

Fig. 3. The effect of different permeant ions on the single channel currents. Single channel currents with different cations from an outside-out patch of an HEK 293 cell at −120 mV. The currents were activated by 2 μM ATP in the presence of 1 mM extracellular Mg^{2+} and Ca^{2+}. The data were filtered at 5 kHz for currents carried by alkali metal ions and 1 kHz for currents carried by organic ions (due to the small amplitudes) and digitized at 10 kHz. The channel openings with the organic ions as charge carriers are almost invisible due to the small amplitude. Note that the scale bar of current amplitude is 5 pA for alkali metal ions and 1 pA for organic ions.

channel block by the ions. The channel selects very strongly for alkali metal ions over organic ions.

The relative permeability of the channel for different ions was taken as the ratio of currents at constant voltage under bi-ionic conditions (Table). The alkali ions permeate an order of magnitude faster than the organic ions despite the similar Stokes radii. The *Stokes* radius of TMA^+ is smaller than Li^+ so the steric sieving can't explain the differences. Non-ionic interactions of the organic ions with the channel (hydrophobic ?) must account for the differences.

The conversion of current to conductance requires a driving force, usually taken to be of the form of Eq. 1. However, since the *I/V* curve is inwardly rectifying, a single value of slope conductance can't apply, but for a sense of scale to literature values we have calculated a conductance at −120 mV based upon estimates of the reversal potential. Our whole cell recordings showed that the reversal potential for alkali metal ions was similar to Na^+ (0 mV), shifted by a small liquid junction potential (<5 mV, *data not shown*). Similarly, Brake et al. (1994) reported that the replacement of extracellular Na^+ by K^+ did not affect the reversal potential of $P2X_2$ whole cell currents, suggesting the Na^+ and K^+ have similar permeability near 0 mV. Thus, for calculating single channel conductances of the alkali ions far from the reversal potential, we assumed the reversal potentials were zero. Since it was impossible to measure reversal potentials for the organic ions from single channel currents, we used the published values from whole cell recording, (Evans et al., 1996) assuming that (intracellular) Na^+ and K^+ had essentially the same permeability. The reversal potentials for $NMDG^+$, $Tris^+$, and TEA^+ were −86, −44 and −79 mV, respectively. The reversal potential for TMA^+ was not available, but taken to be that of TEA. As shown in the Table, the chord conductances of the alkali metal ions at −120 mV were between 30 and 50 pS, while those of the organic ions were 3 ~ 10 pS. The mean currents and excess noise are shown in Fig. 4*A*.

The permeation sequence for the alkali metal ions

Table. Ionic and permeability properties of cations and $P2X_2$ receptors

Cation	Limiting molar conductivity λ_i	*Stokes* radius a (Å)	Amplitude *i* (pA)	Relative permeability	Conductance *G* (pS)
	(mS/M)			P_i/P_{Na}	
K^+	73.50	1.10	5.86	1.40	48.8
Rb^+	77.81	1.05	5.63	1.35	46.9
Cs^+	77.30	1.06	5.36	1.28	44.7
Na^+	50.10	1.63	4.18	1.00	34.8
Li^+	38.68	2.16	3.48	0.83	29.0
$NMDG^+$	24.05	3.37	0.36	0.086	8.8
$Tris^+$	25.50	3.21	0.34	0.081	4.5
TMA^+	44.92	1.82	0.18	0.043	4.4
TEA^+	32.66	2.50	0.16	0.038	3.9

The data of the limiting conductivity of different ions were taken from Castellan (1983) except that $NMDG^+$ was from Barry (1995). The amplitudes were obtained from the data of Fig. 3. The permeability ratios P_i/P_{Na} were calculated from the Goldman-Hodgkin-Katz current equation under bi-ionic conditions as the ratio of the currents. The conductances were calculated by Eq. 1, assuming the reversal potential of alkali metal ions was zero (*see* text). The reversal potentials of organic ions were taken from Evans et al. (1996): −86, −44 and −79 mV for $NMDG^+$, $Tris^+$, and TEA^+, respectively. The conductance of TMA currents was calculated assuming the same reversal potential as TEA. The liquid junction potentials were not corrected since they were only a few mV (Barry & Lynch, 1991; Ng & Barry, 1995).

was $K^+ > Rb^+ > Cs^+ > Na^+ > Li^+$, which is *Eisenman* sequence IV, slightly different from the mobility sequence of ions in free aqueous solution, and characteristic of a binding site of weak-field-strength. Figure 4*B* shows a strong positive correlation between the *Stokes* radius and the relative single channel conductances of the alkali metal ions.

Open Channel Block by Divalent Ions

Figure 5*A* shows the effect of Ca^{2+} on whole cell currents activated by 10 μM ATP at −100 mV. The peak currents decreased with increasing Ca^{2+}. Figure 5*B* shows the fraction of peak current as a function of Ca^{2+} concentration and a fit to the *Woodhull* equation with a dissociation constant K_d of 3.4 mM.

Using outside-out patches, we studied the effect of divalent ions on single channel conductance. Figure 6 show the single channel currents recorded at −120 mV in the presence of different concentrations of extracellular Mg^{2+} (*A*), Ba^{2+} (*B*), Mn^{2+} (*C*) and Ca^{2+} (*D*). The mean amplitudes of the currents decreased with increasing divalent ion concentration, consistent with the idea that divalent ions occasionally block Na^+ permeation. However, the 'buzz mode' kinetic flickering of the open channel appears to be a native property of the channel, independent of the presence of divalent ions (Ding & Sachs, 1999*a*).

To evaluate the concentration dependence of this putative channel block by divalent ions, we measured the mean channel current using *Gaussian* fits to the all-points histogram. The mean open channel currents were fit by the *Woodhull* equation (Eq. 2, Methods) (Woodhull, 1973). As an example, Fig. 7*A* (dotted line) shows the fraction of mean single channel current as a function of Mg^{2+} concentration. The *Woodhull* model yielded an equilibrium dissociation constant, K_d, for Mg^{2+} of 3.9 mM at −120 mV.

All of the divalent ions tested had similar blocking effects on the single channel currents (Table). The equilibrium dissociation constant sequence is $Mn^{2+} < Mg^{2+} < Ca^{2+} < Ba^{2+}$, meaning that Mn^{2+} has the highest affinity for the channel (Fig. 7*B*). Figure 7*B* also shows a positive correlation ($r = 0.91$) between K_d and ionic radius. Assuming all the divalents induce block by binding to the same site, equilibrium selectivity theory (Eisenman & Horn, 1983) suggests that the blocking location is a high field-strength site.

Discussion

Selectivity of Channel Permeation

The single channel K^+ currents have a chord conductance of ~60 pS at −120 mV, and exhibit a flickery behavior similar to the Na^+ currents, i.e., the excess open channel noise has a SD of ~30% of its mean amplitude (Fig. 1). Noise analysis with differential power spectra suggests that the excess open channel noise is caused by confor-

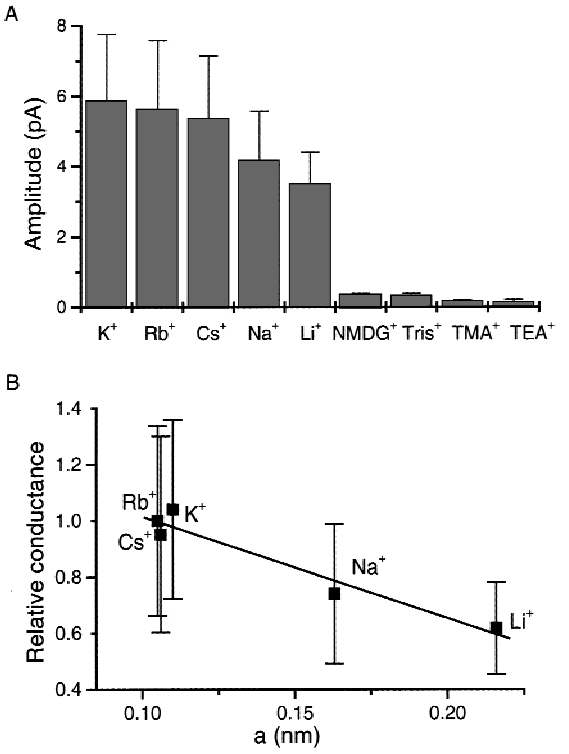

Fig. 4. Summary of the properties of different permeant ions on the single channel current amplitude. (*A*) Single channel current amplitudes of different ions using data from the records in Fig. 3. (*B*) The relative conductance of metal ions as a function of the Stokes radii taken from Castellan (1983) (*see* Table). The single channel conductances (solid points) were normalized to the radius of Rb^+ (smallest). The solid line is a linear fit with a correlation coefficient, $r = 0.97$. According to the Goldman-Hodgkin-Katz (GHK) current equation (Hille, 1992), the current ratio under these bi-ionic conditions is the same as the permeability ratio. The error bars are the excess open-channel noise.

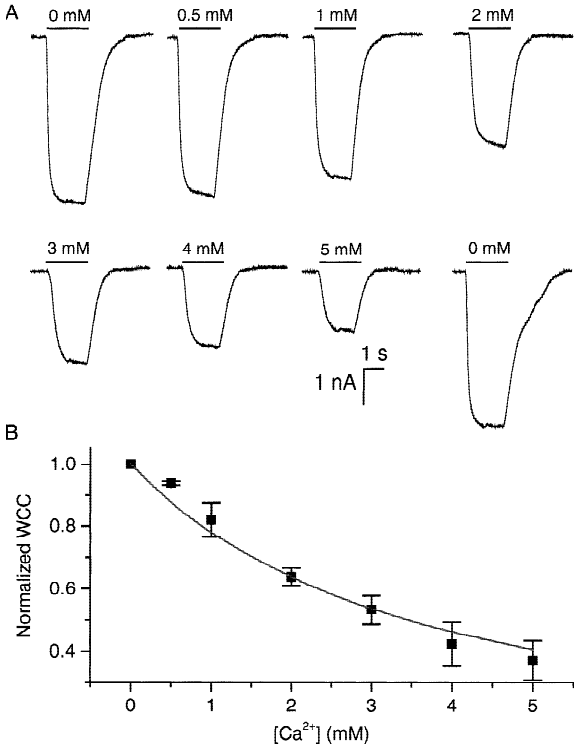

Fig. 5. Whole cell currents carried by Na^+ were blocked by Ca^{2+}. (*A*) The whole cell currents were activated by 2-sec pulses of 10 μM ATP at −100 mV with 140 mM extracellular Na^+ at different extracellular concentrations of Ca^{2+}. The amplitudes appear to be reduced by partial block of channels by Ca^{2+}. The horizontal bars show the duration of ATP/Ca^{2+} application, and the number above them is the concentration of Ca^{2+} in mM. (*B*). The block of WCCs by different concentrations of Ca^{2+}. The solid line is a fit to the *Woodhull* equation (Eq. 2) with a dissociation constant, $K_d = 3.4$ mM ($n = 2$).

mational fluctuations of the channel rather than block by diffusible agents. A detailed study of the noise properties previously has been published (Ding & Sachs, 1999*a*).

$P2X_2$ is strongly selective for alkali metal ions over the organic cations $NMDG^+$, $Tris^+$, TMA^+ and TEA^+. The ionic selectivity for alkali ions, based on the bi-ionic current amplitude, is: $K^+ > Rb^+ > Cs^+ > Na^+ > Li^+$ (Figs. 2 and 3), which is *Eisenman* sequence IV (Hille, 1992). This weak field sequence is consistent with our previous results showing that the single channel conductance has a saturable relationship with Na^+ concentration with an equilibrium constant of 148 mM (Ding & Sachs, 1999*a*).

It is not yet known which residues are involved in the "selectivity filter." Experiments using the substituted cysteine accessibility method (SCAM) (Rassendren et al., 1997) suggest that only residues I328C, N333C, T336C, L338C and D349C in the M2 domain are accessible to MTS reagents. D349 is the only negative residue, possibly constituting a part of the selectivity filter. The negative correlation between the *Stokes* radius of the alkali metal ions and the conductance may be related to a molecular sieve effect or charge density. The small permeability for the organic ions $NMDG^+$, $Tris^+$, TMA^+ and TEA^+ relative to the alkali ions (independent of the *Stokes* radius) suggests that organic ions interact differently with the channel interior.

What are the physical consequences of these conductivity measures? Assuming no specific chemical interactions with the pore and a cylindrical channel geometry, the diameter of the pore region can be estimated from its conductance if the length of channel is known, *c.f.*, (Lichtinger et al., 1998). This calculation is similar to a simple resistivity model (Hille, 1992) but includes finite volume effects as suggested by *Renkin* for the diffusion of neutral molecules through porous filters (Renkin, 1954). The *Renkin* correction factor is reasonable when the rate of entry is the rate-limiting step for permeation and is a limiting case for modeling permeation. The appeal of the model is that when considering relative selectivity, the result is independent of the length of channel.

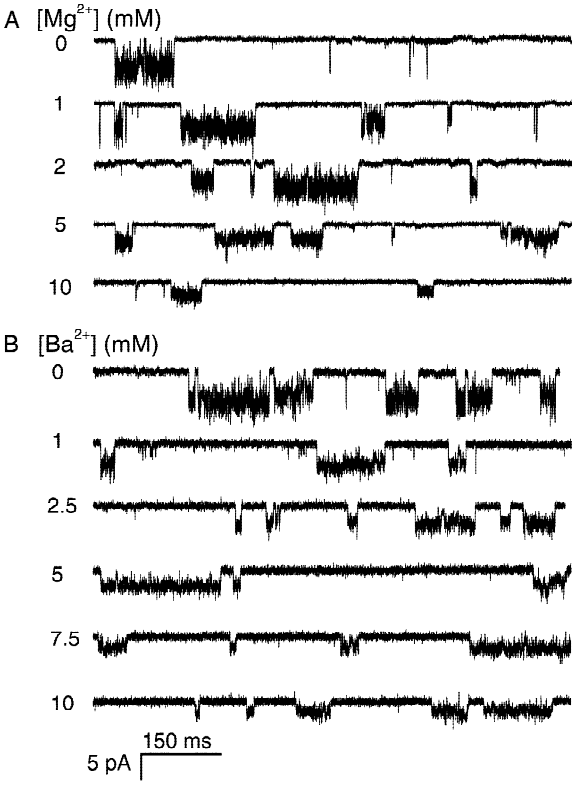

Fig. 6. Block of single channel currents by divalent ions Mg^{2+} (*A*), Ba^{2+} (*B*), Mn^{2+} (*C*) and Ca^{2+} (*D*). The currents were recorded at −120 mV with outside-out patches from HEK 293 cells (*A* and *B*) with 140 mM external Na^+ and *Xenopus* oocytes (*C* and *D*) with 100 mM external Na^+. The currents from oocytes were smaller, due to the lower external Na^+ concentration. The channel amplitudes decreased as the concentration of divalent ions increased. Note that the open channel noise is similar in the presence or in the absence of divalent ions.

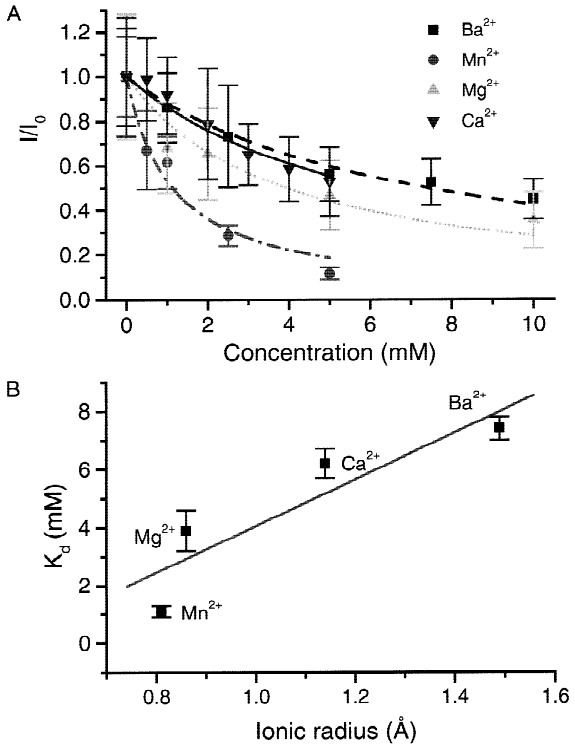

Fig. 7. Block of single channel currents as a function of concentration of divalent ions. (*A*) The mean amplitude of single channel currents relative to zero divalents for Mn^{2+}, Mg^{2+}, Ca^{2+} and Ba^{2+} as a function of divalent ion concentration. The lines are fits of the *Woodhull* equation (Eq. 2) for a single binding site for Mn^{2+} (dash-dot line), Mg^{2+} (dotted line), Ba^{2+} (dashed line) and Ca^{2+} (solid line). The error bars represent the excess open channel noise of the single channel currents. (*B*) The blocking affinity parameters of various divalent ions. The dissociation constants (solid squares) were from the fits of *Woodhull* equation shown in (*A*) and plotted as a function of ionic radii, based on crystallographic data assuming a coordination number of six for each of the metals (Shannon, 1976). The solid line is a linear fit with a correlation coefficient $r = 0.90$.

Although the selectivity sequence of alkali metal ions is not the same as that of aqueous mobility, it approaches that expected for a weak-field site so that the interaction of alkali ions with the channel interior may also be weak. Although K^+, Rb^+, and Cs^+ differ in size and local charge density, their conductances are quite similar. The concentration of ions used for the measurement of conductance (140 mM) is in the linear part of the conductance-concentration curve (Ding & Sachs, 1999*a*), also suggesting that the ions permeate independently. Thus, the alkali metal ions may roughly satisfy the assumptions for the *Renkin* correction factor. According to our data on selectivity and the hydrated radii (i.e., *Stokes* radii) of K^+, Rb^+, Cs^+, Na^+ and Li^+ (Table), and following the method of Lichtinger et al. (1998), the channel is predicted to have a diameter of approximately 2 nm. This diameter is similar to estimates of the cell wall channels from *M. chelonae* (1.8 nm) (Trias et al., 1992) and *C. glutamicum* (2.2 nm) (Lichtinger et al., 1998), but is smaller than that from *M. smegmatis* (3.0 nm) (Trias & Benz, 1994) using the same method of calculation.

However, the conductance of $P2X_2$ channels is much smaller than the conductances of bacterial channels. As previously pointed out, the conductance data do not completely satisfy the assumptions needed for applying the *Renkin* correction factor, and this deviation probably comes from an interaction between the ions and the channel interior. Thus the estimation of pore diameter is probably too large. Crystallography studies have shown that nonselective mechanosensitive channels (MscL) from *M. tuberculosis* have a pore diameter varying from 0.4 to 3.6 nm (Chang et al., 1998). K^+ channels possess a cavity with a 1 nm diameter (Doyle et al., 1998). The pore of the nicotinic ACh channel has been estimated at 0.65 nm from sieving experiments (Dwyer et al., 1980).

Recently two papers reported that $P2X_2$ receptors expressed in oocytes, or HEK 293 cells change their permeability of cations during the prolonged exposure to ATP in whole cell recordings. The channels become

permeable to large molecules such as $NMDG^+$ and dye YO-PRO-1 (Virginio et al., 1999; Khakh et al., 1999). Since there were no single channel measurements in those experiments, and such behavior has never been reported in patches and we did not observe this phenomena in single channel or whole cell recordings, the molecular nature of the phenomenon remains unclear.

Channel Block by Divalent Cations

In both whole cells and outside-out patches, extracellular divalent cations slow the passage of monovalent cations, but this is not the source of the inward rectification since it occurs in the absence of divalent ions (Ding & Sachs, 1999*a*). It is not simple to test whether Ca^{2+} permeates the channel. Fast channel blockers produce brief interruptions of current that may only be detected as an apparent reduction of the open channel amplitudes. Intermediate duration blockers produce visible fluctuations, with durations near the limits of detection (Yellen, 1984). Because of the large open channel fluctuations of $P2X_2$ channels, it is extremely difficult, in practice, to observe new kinetic components resulting from blockade. Under our recording conditions, Ca^{2+}, Mg^{2+}, Ba^{2+} and Mn^{2+} appear to act as fast open channel blockers; the single channel amplitudes are reduced by the divalent ions but the intrinsic flickery behavior remains qualitatively the same. We can't reliably estimate the current carried by divalents, but it appears negligible compared to the Na^+ current.

Divalents can reduce the unitary current by many means, but two simple cases are worth considering: a local blocking effect in the pore or the shielding of fixed charges in the vestibule. If the second mechanism is true, different divalent ions should have the same effect. However, our results show that the effect is different for different divalent species, as previously reported in PC12 cells (Nakazawa & Hess, 1993). Therefore, we prefer the local site model.

We can analyze the characteristics of a blocking site using the *Woodhull* model, and it is simpler to do this ignoring the permeation by Ca^{2+}. The permeability ratio $P_{Ca}{}^{2+}/P_{Na}{}^{+}$ has been reported to be ~2.21 in $P2X_2$ receptors based on reversal potential measurement of whole cell currents (Evans et al., 1996; Virginio et al., 1998). Ca^{2+} permeabilities estimated by whole cell currents may not be reliable since intracellular Ca^{2+} arriving though P2X channels can modulate other conductances and Ca^{2+} will reduce the ATP activity coefficient. Our measurements show that Mn^{+2}, which behaves similarly to other divalents at mM concentrations (Figs. 6 and 7), carries no significant current. In any case, in the concentration range of 0 ~ 10 mM, the current carried by Ca^{2+} appears to be small. The *Woodhull* model of divalent ion block in the pore predicts an affinity of: $Mn^{2+} > Mg^{2+} > Ca^{2+} > Ba^{2+}$ (Fig. 7*B*), similar to the results obtained from PC12 cells (Nakazawa & Hess, 1993). This dissociation constant follows an approximately linear relationship with the ionic radius (Fig. 7*B*), with tighter binding to smaller ions, consistent with interaction with a negatively charged site, possibly D349.

In native receptors, extracellular Ca^{2+} reduces the macroscopic current in a concentration-dependent manner (Nakazawa et al., 1990). We can not rule out the possibility that the decrease in whole-cell currents was caused, at least in part, by a decrease in the activity of free ATP as pointed by Honore et al. (1989). The fact that the dissociation constant from whole cell currents (3.4 mM) is somewhat smaller than that from single channel currents (6.8 mM) may be due to the decrease in free ATP in the presence of divalent ions. Interestingly, we found that in outside-out patches, extracellular divalent ions cause a rapid, cooperative channel inactivation (time constant ~110 msec, *Hill* coefficient ~4) independent of channel block (Ding & Sachs, 1999*b*). This effect seems to be related to a diffusible modulator of the channels that may be involved in pore dilation effects.

We would like to Dr. Annmarie Surprenant (Glaxo and University of Sheffield, UK) for providing stably transfected cell lines. This work was supported by the National Institutes of Health.

References

Abbracchio, M.P., Ceruti, S., Bolego, C., Puglisi, L., Burnstock G., Cattabeni, F. 1996. Trophic roles of P2 purinoceptors in central nervous system astroglial cells. *Ciba Foundation Symposium* **198:**142–147

Akk, G., Auerbach, A. 1996. Inorganic, monovalent cations compete with agonists for the transmitter binding site of nicotinic acetylcholine receptors. *Biophys. J.* **70:**2652–2658

Barry, P.H., Lynch, J.W. 1991. Liquid junction potentials and small cell effects in patch-clamp analysis. *J. Membrane Biol.* **121:**101–117

Benham, C.D. 1990. ATP-gated channels in vascular smooth muscle cells. *Ann. N.Y. Acad. Sci.* **603:**275–285

Benham, C.D. 1992. ATP-gated cation channels in vascular smooth muscle cells. [Review] [23 refs]. *Jpn. J. Pharmacol.* **58:**179P–184P

Benham, C.D., Bouvier, M.M., Evans, M.L. 1991. Changes in cytoplasmic calcium induced by purinergic P2X receptor activation in vascular smooth muscle cells and sensory neurons. *Adv. Exp. Med. Biol.* **304:**229–239

Brake, A.J., Wagenbach, M.J., Julius, D. 1994. New structural motif for ligand-gated ion channels defined by an ionotropic ATP receptor. *Nature* **371:**519–523

Castellan, G.W. 1983. Physical Chemistry. pp. 592–593. Addison-Welsley

Chang, G., Spencer, R.H., Lee, A.T., Barclay, M.T., Rees, D.C. 1998. Structure of the MscL homologue from Mycobacterium tuberculosis: A gated mechanosensitive ion channel. *Science* **282:**2220–2226

Ding, S., Sachs, F. 1999*a*. Single channel properties of $P2X_2$ purinoceptors. *J. Gen. Physiol.* **113:**1–25

Ding, S., Sachs, F. 1999*b*. Inactivation and block of $P2X_2$ receptors by divalent ions. *J. Physiol.* (*in press*)

Doyle, D.A., Cabral, J.M., Pfuetzner, R.A., Kuo, A., Gulbis, J.M., Cohen, S.L., Chait, B., Mackinnon, R. 1998. The structure of the

potassium channel: molecular basis of K^+ conduction and selectivity [see comments]. *Science* **280:**69–77

Dwyer, T.M., Adams, D.J., Hille, B. 1980. The permeability of the endplate channel to organic cations in frog muscle. *J. Gen. Physiol.* **75:**469–492

Eisenman, G., Horn, R. 1983. Ionic selectivity revisited: the role of kinetic and equilibrium processes in ion permeation through channels. *J. Membrane Biol.* **76:**197–225

Evans, R.J. 1996. Single channel properties of ATP-gated cation channels (P2X receptors) heterologously expressed in Chinese hamster ovary cells. *Neurosci. Lett.* **212:**212–214

Evans, R.J., Lewis, C., Virginio, C., Lundstrom K., Buell, G., Surprenant, A., North, R.A. 1996. Ionic permeability of, and divalent cation effects on, two ATP-gated cation channels (P2X receptors) expressed in mammalian cells. *J. Physiol.* **497:**413–422

Fredholm, B.B., Abbracchio, M.P., Burnstock, G., Dubyak, G.R., Harden, T.K., Jacobson, K.A., Schwabe, U., Williams, M. 1997. Towards a revised nomenclature for P1 and P2 receptors. *Trends Pharmacol. Sci.* **18:**79–82

Hamill, O.P., Marty, A., Neher, E., Sakmann, B., Sigworth, F.J. 1981. Improved patch-clamp techniques for high-resolution current recording from cells and cell-free membrane patches. *Pfluegers Arch.* **391:**85–100

Hille, B. 1992. Ionic Channels of Excitable Membranes, 2nd edition. pp. 288–90. Sinauer Associates, Sunderland, MA

Honore, E., Martin, C., Mironneau, C., Mironneau, J. 1989. An ATP-sensitive conductance in cultured smooth muscle cells from pregnant rat myometrium. *Am. J. Physiol.* **257:**C297–C305

Khakh, B.S., Bao X.R., Labarca C., Lester, H.A. 1999. Neuronal P2X transmitter-gated cation channels changed their ion selectivity in seconds. *Nature Neurosci.* **2:**322–330

Krishtal, O.A., Marchenko, S.M., Obukhov, A.G. 1988. Cationic channels activated by extracellular ATP in rat sensory neurons. *Neuroscience* **27:**995–1000

Lichtinger, T., Burkovski, A., Niederweis, M., Kramer, R., Benz, R. 1998. Biochemical and biophysical characterization of the cell wall porin of corynebacterium glutamicum: the channel is formed by a low molecular mass polypeptide. *Biochemistry* **37:**15024–15032

Nakazawa, K., Fujimori, K., Takanaka, A., Inoue, K. 1990. An ATP-activated conductance in pheochromocytoma cells and its suppression by extracellular calcium. *J. Physiol.* **428:**257–272

Nakazawa, K., Hess, P. 1993. Block by calcium of ATP-activated channels in pheochromocytoma cells. *J. Gen. Physiol.* **101:**377–392

Ng, B., Barry, P.H. 1995. The measurement of ionic conductivities and mobilities of certain less common organic ions needed for junction potential corrections in electrophysiology. *J. Neurosci. Meth.* **56:**37–41

Nicke, A., Baumert, H.G., Rettinger, J., Eichele, A., Lambrecht, Mutschler, E., Schmalzing, G. 1998. $P2X_1$ and $P2X_3$ receptors form stable trimers: a novel structural motif of ligand-gated ion channels. *EMBO J.* **17:**3016–3028

North, R.A., Barnard, E.A. 1997. Nucleotide receptors. [Review] [107 refs]. *Curr. Opin. Neurobiol.* **7:**346–357

Rassendren, F., Buell, G., Newbolt, A., North, R.A., Surprenant. 1997. Identification of amino acid residues contributing to the pore of a P2X receptor. *EMBO J.* **16:**3446–3454

Renkin, E.M. 1954. Filtration, diffusion, and molecular sieving through porous cellulose membranes. *J. Gen. Physiol.* **38:**225–243

Rogers, M., Dani, J.A. 1995. Comparison of quantitative calcium flux through NMDA, ATP, and ACh receptor channels. *Biophys. J.* **68:**501–506

Shannon, R.D. 1976. Revised effective ionic radii and systematic studies of interatomic distances in halides and chalcogenides. *Acta Crystallographica* **A32:**751–767

Sivilotti, L.G., McNeil, D.K., Lewis, T.M., Nassar, M.A., Schoepfer, R., Colquhoun, D. 1997. Recombinant nicotinic receptors, expressed in Xenopus oocytes, do not resemble native rat sympathetic ganglion receptors in single-channel behaviour. *J. Physiol.* **500:**123–138

Surprenant, A., Rassendren, F., Kawashima, E., North, R.A., Buell, G. 1996. The cytolytic P2Z receptor for extracellular ATP identified as a P2X receptor ($P2X_7$). *Science* **272:**735–738

Trias, J., Benz, R. 1994. Permeability of the cell wall of Mycobacterium smegmatis. *Mol. Microbiol.* **14:**283–290

Trias, J., Jarlier, V., Benz, R. 1992. Porins in the cell wall of mycobacteria. *Science* **258:**1479–1481

Valera, S., Hussy, N., Evans, R.J., Adami, N., North, R.A., Surprenant, A., Buell, G. 1994. A new class of ligand-gated ion channel defined by P2X receptor for extracellular ATP. *Nature* **371:**516–519

Virginio, C., Surprenant, A., North, R.A. 1998. Calcium permeability and block at homomeric and heteromeric $P2X_2$ and $P2X_3$ receptors, and P2X receptors in rat nodose neurones. *J. Physiol.* **510:**27–35

Virginio, C., Mckkenzie, A, Rassendren F.A., North, R.A., Suprenant, A. 1999. Pore dilation of neuronal P2X receptor channels. *Nature Neurosci.* **2:**315–21

Woodhull, A.M. 1973. Ionic blockage of sodium channels in nerve. *J. Gen. Physiol.* **61:**687–708

Yellen, G. 1984. Ionic permeation and blockade in Ca^{2+}-activated K^+ channels of bovine chromaffin cells. *J. Gen. Physiol.* **84:**157–186.